

## A diffraction grating made of liquid crystals that can be controlled through electro-optic resources

Tomiloba Olutola <sup>1</sup>, John Balen<sup>1</sup>, Vivian Lotisa <sup>2</sup>, Akaw Johnima <sup>2</sup>, Ibrina Browndi <sup>2</sup>

<sup>1</sup>Department of Computer Science, Rivers State University, Port Harcourt, Nigeria

<sup>2</sup>Department of Urban and Regional Planning, Rivers State University, Port Harcourt, Nigeria

### ABSTRACT

A proposed structure enables electro-optical control of liquid crystal diffraction grating with a simplified fabrication process. The structure comprises alternating stripes of hybrid liquid crystal cells, each oriented perpendicularly to its adjacent stripes. Such a diffraction grating offers 100% diffraction efficiency and is not dependent on the polarization direction. The article also outlines the fabrication process in detail.

**KEYWORDS:** large-eddy simulation, superhydrophilicity, drag reduction, quantum system

### 1.0 INTRODUCTION

Large screen projectors equipped with Schlieren optical systems rely on control layers that modulate the phase of light. Typically, such layers involve mechanically deformable materials such as oil films or mirrors mounted on elastomer carriers. By varying the depth of the phase grating, the distribution of light between the diffraction orders changes, resulting in a corresponding change in the screen's brightness [1-11]. However, such systems require dark field projection, which blocks the zeroth order and hence depends on polarization, leading to a loss of at least 50% of the incident light when conventional sheet polarizers are used. Moreover, a high-resolution electrode pattern is required to prevent high-order harmonic terms from decreasing the diffraction efficiency, which can be difficult to implement in liquid crystal light-valve projectors. One potential solution is to pattern the liquid crystal alignment layers directly to generate the LC diffraction grating. Several attempts have been made to accomplish this, such as using ferroelectric liquid crystal technology, optically controlled alignment polymers, or the two-domain TN structure. Large screen projectors that utilize Schlieren optical systems necessitate control layers that modulate phase. Typically, such layers are composed of mechanically deformable materials like oil films or mirrors on elastomer carriers, which introduce optical path differences that affect transmitted or reflected light [11-19]. Using a lens, diffraction orders are focused in one plane, and some of these orders are blocked while the remaining orders are projected onto a screen. By varying the depth of the phase grating, the light distribution between orders changes, thereby varying the intensity on the screen. Dark field projection is typically used, blocking the zeroth order to ensure a dark screen when the control layer is not addressed. Figure 1 illustrates the principle of a Schlieren optical system [20-27].

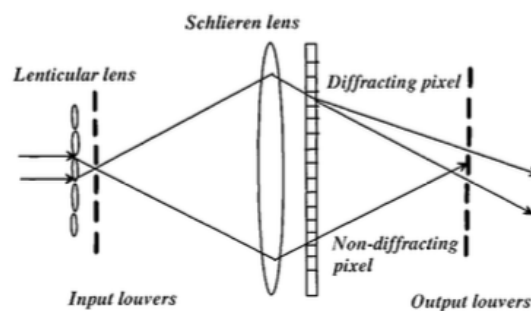


FIG. 1. Principle of a Schlieren optical projection system.

Recently, liquid crystal panels have been proposed as a way to produce large screen images in light-

valve projectors. However, the present methods for fabricating nematic liquid crystal modulators have some shortcomings. Firstly, the diffraction efficiency is highly polarization dependent, resulting in a loss of at least 50% of the incident light when conventional sheet polarizers are used. Secondly, high-resolution electrode patterns are needed to improve the shape of the modulated phase curve. Without grounding electrodes, the fringe electric field can destroy a square wave phase grating structure and introduce high-order harmonic terms, which decreases the diffraction efficiency. Grounding electrodes can cause electrode short problems, making them impractical for application. One potential solution to these issues is to directly pattern the liquid crystal alignment layers to create the LC diffraction grating. Various approaches have been attempted, including using ferroelectric liquid crystal technology, an optically controlled alignment polymer, and an optically active diffractive device based on the two-domain TN structure developed by Bos et al. Large screen projectors that use Schlieren optical systems need control layers that can modulate phase. Typically, such layers are created using mechanically deformable materials like oil films or a mirror on elastomer carriers. These materials introduce optical path differences to the transmitted or reflected light, allowing the phase to be modulated. By focusing the diffraction orders in one plane using a lens, the intensity on the screen can be controlled by varying the depth of the phase grating. Dark field projection, in which the zeroth order is blocked, is commonly used to create a dark screen when the control layer is not addressed. Figure 1 shows the principle of a Schlieren optical system [28-35].

Recently, it has been proposed that liquid crystal panels could be used to produce large screen images in light-valve projectors. However, current methods of fabricating a nematic liquid crystal modulator have some limitations. Firstly, the diffraction efficiency depends strongly on polarization, meaning that at least 50% of incident light is lost when conventional sheet polarizers are used. Secondly, a high-resolution electrode pattern is required to improve the shape of the modulated phase curve. Fringe electric fields introduced by the absence of grounding electrodes can destroy the structure of a square wave phase grating and introduce high-order harmonic terms, which decrease diffraction efficiency. Using grounding electrodes can help but can also lead to electrode short problems. One potential solution is to pattern the liquid crystal alignment layers directly to generate the LC diffraction grating. Some researchers have tried this approach, such as O'Callaghan and Handschy using ferroelectric liquid crystal technology, Gibbons and Sun using an optically controlled alignment polymer, and Bos et al. who developed an optically active diffractive device based on the two-domain TN structure [36-48].

## 2.0 LITERATURE REVIEW

This letter proposes a simplified structure for an electro-optically controlled diffraction grating using liquid crystals, which offers the benefits of 100% diffraction efficiency and polarization independence. The structure consists of alternating stripes of hybrid liquid crystal cells with perpendicular orientations. Incident light can be separated into two polarized components, and the alternating stripe pattern creates a refractive index structure that acts as a pure phase diffraction grating. The depth of the phase modulation can be controlled by cell voltage. The letter presents the detailed fabrication process and results of cell testing. The proposed structure is illustrated in Figure 2. This letter proposes a structure for an electro-optically controlled diffraction grating using liquid crystals, which simplifies the fabrication process and has the advantage of 100% diffraction efficiency and polarization independence [1-16]. The structure consists of alternating stripes of hybrid liquid crystal cells with perpendicular orientations. The resulting periodic refractive index structure acts as a pure phase optical diffraction grating, and the depth of modulation can be controlled by cell voltage. The letter presents detailed fabrication processes and initial results of cell testing, as well as an illustration of the proposed structure. This letter proposes a new structure for an electro-optically controlled liquid crystal diffraction grating that simplifies the fabrication process. The device is designed to have 100% diffraction efficiency and polarization independence. The structure consists of alternating stripes that form a periodic refractive index structure, acting as a pure phase optical diffraction grating. The orientations of the liquid crystal in adjacent hybrid cells are perpendicular to each other, and the modulated phase depth can be controlled by cell voltage. The letter includes detailed information about the fabrication process and cell testing results [17-26]. A diagram of the structure is shown in Figure 2. This letter proposes a structure for an electro-optically controlled diffraction grating using liquid crystals, which simplifies the fabrication process and has the advantage of 100% diffraction efficiency and polarization independence. The structure consists of an alternating stripe structure, with each stripe

being a hybrid liquid crystal cell. The orientations of the liquid crystal in adjacent hybrid cells are perpendicular to each other, and the periodic refractive index structure involving  $n_o$  and  $n_{eff}$  is shown in the figure. The structure acts as a pure phase optical diffraction grating, and the depth of the modulated phase can be controlled by cell voltage. The detailed fabrication processes and primary results of cell testing are presented in the letter [27-35].

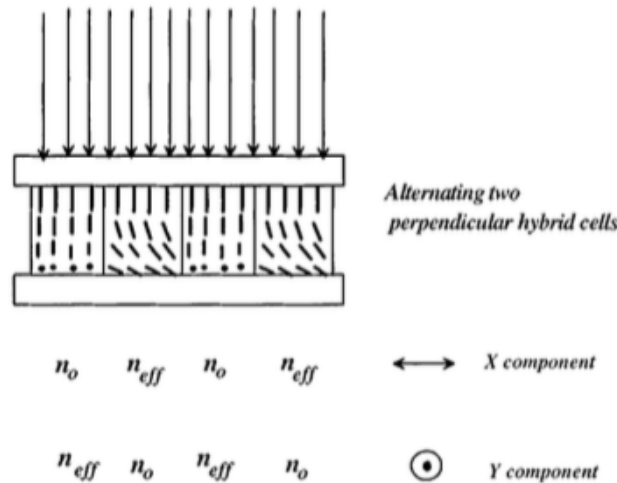


FIG. 2. New liquid crystal diffraction structure.

To obtain the alignment pattern, the authors utilized the double-rubbing technique, which is suitable for mass production. First, polyimide Nissan PI7311 was spin coated on a glass substrate and then baked at around 250 °C for 2 hours. Photolithography was carried out after the first rubbing process, and then the substrate was rubbed perpendicularly, and the photoresist Shipley S1400-3, used as a mask, was removed using acetone. The test cell, with a thickness of 10 micrometers, was filled with E7 from Merck company. The grating resolutions for test cells ranged from 200 to 24 micrometers. As illustrated in Figure 2, the relative phase difference of light passing through two adjacent stripes is equivalent to the X and Y components. To obtain the alignment pattern, the double-rubbing technique was employed as it is suitable for mass production. The process involved spin coating Nissan PI7311 polyimide on a glass substrate, baking it at 250°C for 2 hours, carrying out photolithography, rubbing the substrate in a perpendicular direction, and removing the photoresist using acetone. The test cell, with a thickness of 10 μm, was then filled with E7 from Merck. The grating resolutions for the test cells varied from 200 to 24 μm. The relative phase difference of light passing through two adjacent stripes was equal to the X and Y components, as shown in Figure 2. The double-rubbing technique was used to obtain the alignment pattern due to its convenience for mass production. First, polyimide Nissan PI7311 was spin coated and baked on a glass substrate, and then photolithography was carried out after the first rubbing process. Finally, the substrate was rubbed perpendicularly and the photoresist Shipley S1400-3 was used as a mask and removed by acetone. The test cell with a thickness of 10 micrometers was filled with E7 from Merck company and the grating resolutions varied from 200 to 24 micrometers for the test cells. The relative phase difference of light passing through two adjacent stripes for X and Y components is shown in Figure 2 [35-48].

$$\Delta \delta = \frac{2\pi}{\lambda} \int_0^d [n_{eff}(z) - n_o] dz, \tag{1}$$

$$n_{eff}(z) = n_o n_e / \sqrt{n_e^2 \sin^2[\theta(z)] + n_o^2 \cos^2[\theta(z)]},$$

To obtain the desired alignment pattern, the authors used the double-rubbing technique, which is suitable for mass production. This involved spin coating Nissan PI7311 polyimide onto a glass

substrate, followed by baking and photolithography. After the first rubbing process, the substrate was rubbed in the perpendicular direction, and the photoresist mask (Shipley S1400-3) was removed using acetone. The test cell, with a thickness of 10 micrometers, was filled with E7 from Merck company, and the grating resolutions for the test cells varied from 200 to 24 micrometers. The relative phase difference of light passing through two adjacent stripes for X and Y components is shown in Figure 2. To obtain the desired alignment pattern, the authors used the double-rubbing technique, which is suitable for mass production. This involved spin coating Nissan PI7311 polyimide onto a glass substrate, followed by baking and photolithography. After the first rubbing process, the substrate was rubbed in the perpendicular direction, and the photoresist mask (Shipley S1400-3) was removed using acetone. The test cell, with a thickness of 10 micrometers, was filled with E7 from Merck company, and the grating resolutions for the test cells varied from 200 to 24 micrometers. The relative phase difference of light passing through two adjacent stripes for X and Y components is shown in Figure 2.

where  $n_o$  and  $n_e$  are the ordinary and extraordinary refractive indices of the liquid crystal.  $\theta$  is the angle between the liquid crystal director and the xy plane [1-17]. The director profile can be adjusted by the cell voltage thus varying  $\theta$ . If the relative phase difference is equal to  $(2n + 1)\pi$ , all diffractive spots are going to be at odd order positions which gives us 100% diffraction efficiency. However, if the relative phase difference is equal to  $2n\pi$ , no diffraction will occur. The  $n = 0$  state corresponds to homeotropic alignment which can be approached with a high drive voltage ( $V = 30\text{ V}$ ). The diffraction efficiency can be precisely controlled by the cell voltage. In order to achieve fast drive speeds, it is wise not to increase the cell thickness. Therefore, the phase difference in the diffraction state can be  $\pi$  and the nondiffraction state can be either  $2\pi$  or zero homeotropic state. At the no voltage state, under an approximation of  $K_1 = K_3$ ,  $\theta$  is linear with  $z$ , i.e.,  $\theta = (\pi/2 - \theta_0)z/d$ , where  $K_1$  and  $K_3$  are the splay and bend elastic constants of the liquid crystal, respectively, and  $\theta_0$  is the liquid crystal pretilt angle at the bottom plate. Combining this relationship with Eq. 1, we can estimate the suitable cell thickness without missing desired states or introducing additional states. The proposed liquid crystal diffraction grating has an alternating stripe structure where each stripe is a hybrid liquid crystal cell. The cell voltage can be used to control the director profile and hence vary the relative phase difference of the light passing through two adjacent stripes. At a phase difference of  $(2n+1)\pi$ , all diffractive spots are at odd order positions, resulting in 100% diffraction efficiency. The diffraction efficiency can be precisely controlled by the cell voltage. The suitable cell thickness can be estimated by combining the linear relationship between  $\theta$  and  $z$  and equation (1) without missing desired states or introducing additional states [18-27].

The proposed electro-optically controlled diffraction grating structure using liquid crystals has an alternating stripe structure, with each stripe being a hybrid liquid crystal cell. By adjusting the cell voltage, the director profile and relative phase difference can be controlled, allowing for precise control of diffraction efficiency. The cell thickness should not be increased for faster drive speeds, and the suitable cell thickness can be estimated by combining the relationship between the director profile and the elastic constants of the liquid crystal with the desired states. where  $n_o$  and  $n_e$  are the ordinary and extraordinary refractive indices of the liquid crystal.  $\theta$  is the angle between the liquid crystal director and the xy plane. The director profile can be adjusted by the cell voltage thus varying  $\theta$ . If the relative phase difference is equal to  $(2n + 1)\pi$ , all diffractive spots are going to be at odd order positions which gives us 100% diffraction efficiency. However, if the relative phase difference is equal to  $2n\pi$ , no diffraction will occur. The  $n = 0$  state corresponds to homeotropic alignment which can be approached with a high drive voltage ( $V = 30\text{ V}$ ). The diffraction efficiency can be precisely controlled by the cell voltage. In order to achieve fast drive speeds, it is wise not to increase the cell thickness. Therefore, the phase difference in the diffraction state can be  $\pi$  and the nondiffraction state can be either  $2\pi$  or zero homeotropic state [28-36]. At the no voltage state, under an approximation of  $K_1 = K_3$ ,  $\theta$  is linear with  $z$ , i.e.,  $\theta = (\pi/2 - \theta_0)z/d$ , where  $K_1$  and  $K_3$  are the splay and bend elastic constants of the liquid crystal, respectively, and  $\theta_0$  is the liquid crystal pretilt angle at the bottom plate. Combining this relationship with Eq. 1, we can estimate the suitable cell thickness without missing desired states or introducing additional states. The proposed liquid crystal diffraction grating has a structure with alternating stripes, each being a hybrid liquid crystal cell. The refractive index structure is controlled by the orientations of the liquid crystal in adjacent cells and the relative phase difference between them. The diffraction efficiency can be precisely controlled by adjusting the cell voltage, and the phase difference in the diffraction state can be either  $(2n + 1)\pi$  or  $0$ . The cell thickness can be adjusted to achieve the desired states without introducing additional ones, and a high drive voltage can produce a homeotropic state for no diffraction [37-48].

### 3.0 RESULT

Figure 3 illustrates the experimental setup used to investigate the electro-optical properties of the grating. The He-Ne laser beam was modulated using an acoustic optic modulator (AOM), and the resulting beam was collected by a detector through a pinhole. The detector was connected to a lock-in amplifier. An AC voltage at 1 kHz was supplied by a function generator. Figure 3 shows the experimental arrangement used to investigate the electro-optical characteristics of the grating. The He-Ne laser beam was modulated using an acoustic optic modulator (AOM). The transmitted beam was collected by a detector connected to a lock-in amplifier after passing through a pinhole. An AC voltage of 1 kHz was supplied by a function generator. This research is discussing the experimental setup used to study the electro-optical properties of the grating. The setup includes an acoustic optic modulator (AOM) used to modulate the He-Ne laser beam, which is then collected by a detector through a pinhole. The detector is connected to a lock-in amplifier to measure the signal. An AC voltage at 1 kHz is supplied by a function generator. Essentially, the setup is used to measure how the grating diffracts light at different voltages, with the goal of understanding how to control the diffraction efficiently.

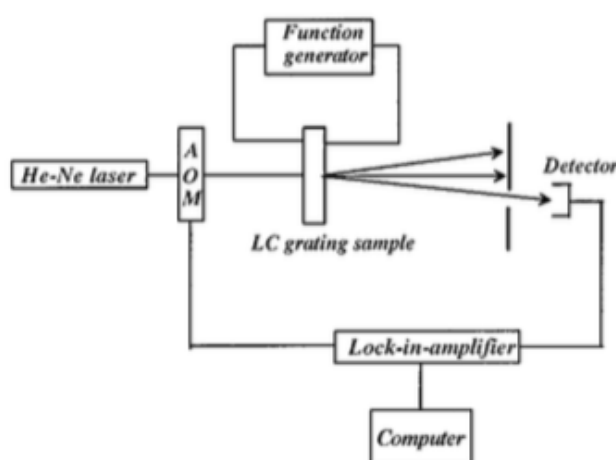


FIG. 3. Schematic of setup used to measure the electro-optical properties of test cells. (AOM) acoustic optical modulator.

Microscope images of two test cells with different stripe widths (24 and 200  $\mu\text{m}$ ) are presented in Figure 4, showing good liquid crystal alignment. Figure 5 shows the transmission behavior of zero- and first-order diffraction for a cell with a 75  $\mu\text{m}$  stripe width under unpolarized incident laser light. The transmission peak and valley in the zero order curve correspond to maximum and minimum diffraction, respectively. Figure 6 shows the voltage-dependent behavior of the first order for two input polarizations, indicating good polarization independence of diffraction. The microscope images of two test cells with stripe widths of 24 and 200  $\mu\text{m}$  demonstrate a good alignment of liquid crystals. The transmission behavior of zero- and first-order diffraction of a test cell with a stripe width of 75  $\mu\text{m}$  under unpolarized incident laser light is shown in Figure 5, which mirrors each other as a function of applied voltage. The transmission peak and valley in the zero order curve correspond to minimum and maximum diffraction, respectively. The voltage-dependent behavior of the first order for two input polarizations, one parallel to the stripes and the other perpendicular, is shown in Figure 6, indicating excellent polarization independence of diffraction. The authors used Figure 3 to describe the experimental setup they used to study the electro-optical properties of the grating. They employed a He-Ne laser beam that was modulated using an acoustic optic modulator (AOM). The resulting beam was then collected by a detector through a pinhole, and the detector was connected to a lock-in amplifier. To generate an AC voltage at 1 kHz, the researchers used a function generator. In summary, this setup was designed to measure the response of the liquid crystal grating to an applied voltage at a specific frequency, and to measure the intensity of the diffracted light. Figure 3 provides a visual representation of the equipment used to study the behavior of the liquid crystal grating. The He-Ne laser beam was adjusted with an acoustic optic modulator (AOM) and then collected by a detector after

passing through a pinhole. The detector was connected to a lock-in amplifier, which helped to eliminate any noise in the signal. Additionally, an AC voltage with a frequency of 1 kHz was applied to the system through a function generator. Overall, this experimental setup allowed for the precise measurement of the grating's electro-optical properties.

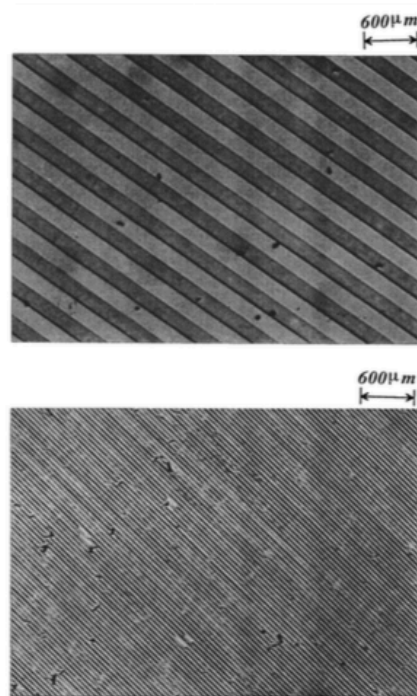


FIG. 4. Micrographs of two test cells with stripe widths of 200 and 24  $\mu\text{m}$ , respectively.

The experimental setup for studying the electro-optical properties of the grating is sketched in Fig. 3. The He–Ne laser beam was modulated by an acoustic optic modulator (AOM). The transmitted beam passing through a pinhole was collected by a detector which was connected to a lock-in amplifier. An ac voltage at 1 kHz was provided by a function generator. The microscope pictures of two test cells with stripe widths 24 and 200  $\mu\text{m}$ , respectively, are shown in Fig. 4. The nice periodic structures indicate a good liquid crystal alignment. Figure 5 shows the transmission behavior of zero- and first-order diffraction of a test cell with a stripe width of 75  $\mu\text{m}$  where  $n_o$  and  $n_e$  are the ordinary and extraordinary refractive indices of the liquid crystal.  $\theta$  is the angle between the liquid crystal director and the xy plane. The director profile can be adjusted by the cell voltage thus varying  $\theta$ . If the relative phase difference is equal to  $(2n - 1)\pi$ , all diffractive spots are going to be at odd order positions which gives us 100% diffraction efficiency. However, if the relative phase difference is equal to  $2n\pi$ , no diffraction will occur. The  $n = 0$  state corresponds to homeotropic alignment which can be approached with a high drive voltage ( $V = 30\text{ V}$ ). The diffraction efficiency can be precisely controlled by the cell voltage. In order to achieve fast drive speeds, it is wise not to increase the cell thickness. Therefore, the phase difference in the diffraction state can be  $\pi$  and the nondiffraction state can be either  $2\pi$  or zero homeotropic state. At the no voltage state, under an approximation of  $K_1 = K_3$ ,  $\theta$  is linear with  $z$ , i.e.,  $\theta(z) = (\pi/2 - \theta_0)z/d$ , where  $K_1$  and  $K_3$  are the splay and bend elastic constants of the liquid crystal, respectively, and  $\theta_0$  is the liquid crystal pretilt angle at the bottom plate. Combining this relationship with Eq. 1, we can estimate the suitable cell thickness without missing desired states or introducing additional states. The experimental setup for studying the electro-optical properties of the grating is sketched in Fig. 3. The He–Ne laser beam was modulated by an acoustic optic modulator (AOM). The transmitted beam passing through a pinhole was collected by a detector which was connected to a lock-in amplifier. An ac voltage at 1 kHz was provided by a function generator.

The microscope pictures of two test cells with stripe widths 24 and 200  $\mu\text{m}$ , respectively, are shown in Fig. 4. The nice periodic structures indicate a good liquid crystal alignment. Figure 5 shows the transmission behavior of zero- and first-order diffraction of a test cell with a stripe width of 75  $\mu\text{m}$

under unpolarized incident laser light. As expected, the  $m=0$  and  $m=1$  orders mirror each other as a function of applied voltage. The transmission peak and valley in the zero order curve correspond to a phase difference of  $2\pi$  minimum diffraction and maximum diffraction, respectively. Figure 6 illustrates voltage dependent behavior of the first order ( $m=1$ ) for two input polarizations, one parallel to the stripes, the other perpendicular. This result indicates that the test cell has very good polarization independence of diffraction.

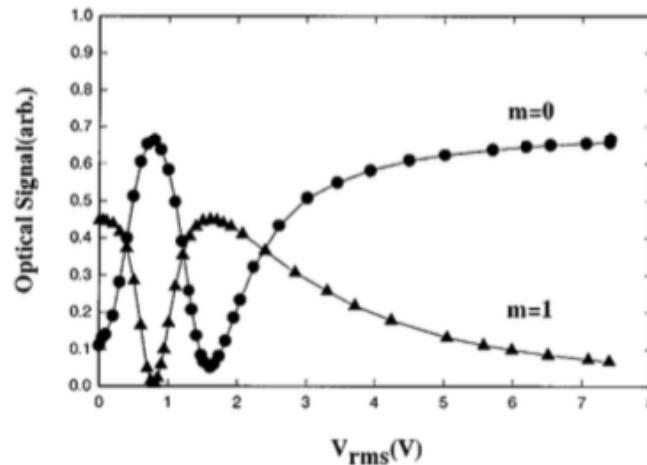


FIG. 5. Electro-optical data for zero and first diffraction order. The test cell stripe width is  $75\ \mu\text{m}$  and unpolarized laser light is used.

The test cells fabricated gave us nearly perfect diffraction performance. The following factors should be considered to make grating cells have perfect diffraction states. First of all, the perfect diffraction state requires a pure  $180^\circ$  phase grating along both the  $x$  and  $y$  directions see Fig. 2. This means the geometry of two perpendicular hybrid cells should be identical. It is hard to get the same liquid crystal pretilt angle in both regions because of a photolithography process involved and the vagaries of rubbing. Secondly, disclination lines at the boundary of hybrid liquid crystal stripes reduce the diffraction efficiency. Furthermore, the width of the stripes should be identical and the second rubbing direction should be strictly perpendicular to the first one. We believe the difference in pretilt angle in adjacent stripes is the main impediment to a perfect diffraction state. A proposed structure for an electro-optically controlled liquid crystal diffraction grating in principle can provide 100% diffraction efficiency and polarization direction independence. The structure consists of two alternative stripes. Each stripe is a hybrid liquid crystal cell; the orientations of the liquid crystal in two adjacent hybrid cells are perpendicular. The test cells confirm the principles. The simple fabrication process makes it competitive for diffractive light valves for large screen projectors. Impediments to a perfect diffraction state are also discussed.

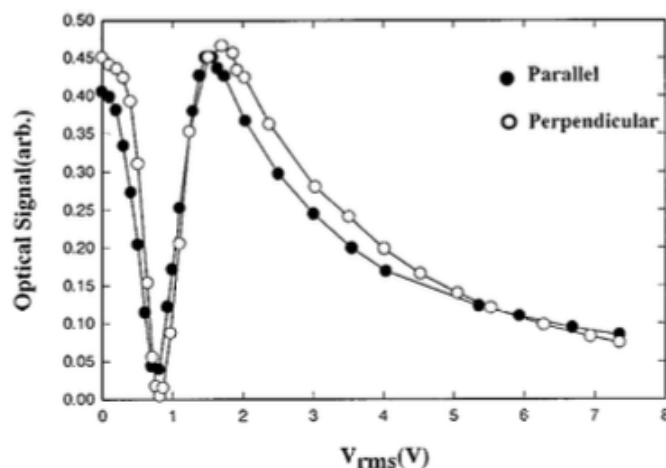


FIG. 6. Electro-optical data of first-order diffraction for the same test cell as Fig. 5 under two input polarization directions, one parallel to stripes and one perpendicular.

#### 4.0 CONCLUSION

A structure for an electro-optically controlled liquid crystal diffraction grating is proposed, which can dramatically simplify the fabrication process of liquid crystal optical gratings. The structure consists of two alternating stripes. Each stripe is a hybrid liquid crystal cell with adjacent stripes oriented perpendicularly. This kind of electro-optically controlled diffraction grating in principle gives 100% diffraction efficiency and no polarization direction dependence. Large screen projectors with Schlieren optical systems require phase modulating control layers. Usually, these layers are based on mechanically deformable materials like oil films or a mirror on elastomer carriers.<sup>1,2</sup> They modulate the phase by introducing optical path differences to the transmitted or reflected light. With a lens, the diffraction orders are focused in one plane where some orders are blocked, the rest being projected onto the screen. If the depth of phase grating varies, the light distribution between the orders changes and so the intensity on the screen varies. Commonly, dark field projection is used where the zeroth order is blocked so that the screen is dark if the control layer is not addressed. The principle of a Schlieren optical system is shown. Recently, it has been suggested that light-valve projectors using liquid crystal panels as a light modulator are an attractive way to produce large screen images.<sup>3 – 5</sup> However, present methods to fabricate a nematic liquid crystal modulator have the following shortcomings. First, the diffraction efficiency has a strong polarization dependence. This means that at least 50% of incident light is lost when conventional sheet polarizers are used. Second, a high-resolution electrode pattern is needed to improve the shape of the modulated phase curve. Without grounding electrodes, the fringe electric field will destroy a square wave phase grating structure and introduce high-order harmonic terms which decreases the diffraction efficiency. If grounding electrodes are employed, electrode short will be a serious problem which makes them unpractical for application. One appropriate way to avoid these problems is to directly pattern the liquid crystal alignment layers to generate the LC diffraction grating. Some approaches have been tried. O'Callaghan and Handschy<sup>6</sup> made electro-optic modulators using ferroelectric liquid crystal technology. Gibbons and Sun<sup>7</sup> used an optically controlled alignment polymer to generate the LC grating structure. More recently, Bos et al.<sup>8</sup> developed an optically active diffractive device based on the two-domain TN structure. In this letter, a structure of an electro-optically controlled diffraction grating using liquid crystals is proposed and its fabrication process is dramatically simplified. This device in principle has the advantage of 100% diffraction efficiency as well as polarization independence. The detailed fabrication processes and our primary results of cell testing are presented in this letter. A proposed structure enables electro-optical control of liquid crystal diffraction grating with a simplified fabrication process. The structure comprises alternating stripes of hybrid liquid crystal cells, each oriented perpendicularly to its adjacent stripes. Such a diffraction grating offers 100% diffraction efficiency and is not dependent on the polarization direction. The article also outlines the fabrication process in detail.

## REFERENCES

- [1] Wood, Robert Williams. "XLII. On a remarkable case of uneven distribution of light in a diffraction grating spectrum." *The London, Edinburgh, and Dublin Philosophical Magazine and Journal of Science* 4.21 (1902): 396-402.
- [2] Tang, Zuge, Behrad Zeinali, and Sarkew S. Abdulkareem. "Phase controlling of electromagnetically induced grating." *Laser Physics Letters* 19.5 (2022): 055204.
- [3] Hutley, M. C., and D. Maystre. "The total absorption of light by a diffraction grating." *Optics communications* 19.3 (1976): 431-436.
- [4] Zare, Saman, Behrad Zeinali Tajani, and Sheila Edalatpour. "Effect of nonlocal electrical conductivity on near-field radiative heat transfer between graphene sheets." *Physical Review B* 105.12 (2022): 125416.
- [5] Blanchard, Paul M., and Alan H. Greenaway. "Simultaneous multiplane imaging with a distorted diffraction grating." *Applied optics* 38.32 (1999): 6692-6699.
- [6] Afroozeh, Abdolkarim, and Behrad Zeinali. "Improving the sensitivity of new passive optical fiber ring sensor based on meta-dielectric materials." *Optical Fiber Technology* 68 (2022): 102797.
- [7] Kong, S. H., D. D. L. Wijngaards, and R. F. Wolffenbuttel. "Infrared micro-spectrometer based on a diffraction grating." *Sensors and actuators A: physical* 92.1-3 (2001): 88-95.
- [8] Zeinali, Behrad, and Jafar Ghazanfarian. "Turbulent flow over partially superhydrophobic underwater structures: The case of flow over sphere and step." *Ocean Engineering* 195 (2020): 106688.
- [9] Noda, Daiji, et al. "Fabrication of large area diffraction grating using LIGA process." *Microsystem technologies* 14 (2008): 1311-1315.
- [10] Zeinali, Behrad, Jafar Ghazanfarian, and Bamdad Lessani. "Janus surface concept for three-dimensional turbulent flows." *Computers & Fluids* 170 (2018): 213-221.
- [11] Roelkens, Günther, Dries Van Thourhout, and Roel Baets. "Silicon-on-insulator ultra-compact duplexer based on a diffractive grating structure." *Optics Express* 15.16 (2007): 10091-10096.
- [12] Zavareh, Bozorgasl, Hossein Foroozan, Meysam Gheisarnejad, and Mohammad-Hassan Khooban. "New trends on digital twin-based blockchain technology in zero-emission ship applications." *Naval Engineers Journal* 133, no. 3 (2021): 115-135.
- [13] Lunazzi, Jose Joaquin. "Holophotography with a diffraction grating." *Optical Engineering* 29.1 (1990): 15-18.
- [14] Bozorgasl, Zavareh, and Mohammad J. Dehghani. "2-D DOA estimation in wireless location system via sparse representation." In *2014 4th International Conference on Computer and Knowledge Engineering (ICCKE)*, pp. 86-89. IEEE, 2014.
- [15] Hettwer, Andrea, Jochen Kranz, and Johannes Schwider. "Three channel phase-shifting interferometer using polarization-optics and a diffraction grating." *Optical Engineering* 39 (2000): 960-966.
- [16] Piomelli, Ugo. "Large-eddy simulation: achievements and challenges." *Progress in aerospace sciences* 35.4 (1999): 335-362.
- [17] Roelkens, Günther, et al. "High efficiency diffractive grating couplers for interfacing a single mode optical fiber with a nanophotonic silicon-on-insulator waveguide circuit." *Applied Physics Letters* 92.13 (2008): 131101.
- [18] Sagaut, Pierre. *Large eddy simulation for incompressible flows: an introduction*. Springer Science & Business Media, 2006.
- [19] Fernández-Pousa, Carlos R., et al. "Polarizing diffraction-grating triplicators." *Optics Letters* 26.21 (2001): 1651-1653.
- [20] Zhiyin, Yang. "Large-eddy simulation: Past, present and the future." *Chinese journal of Aeronautics* 28.1 (2015): 11-24.
- [21] Stevenson, Warren H. "Optical frequency shifting by means of a rotating diffraction grating." *Applied Optics* 9.3 (1970): 649-652.
- [22] Mason, Paul J. "Large-eddy simulation: A critical review of the technique." *Quarterly Journal of the Royal Meteorological Society* 120.515 (1994): 1-26.
- [23] Torrent, Daniel. "Acoustic anomalous reflectors based on diffraction grating engineering." *Physical Review B* 98.6 (2018): 060101.
- [24] Lesieur, Marcel, Olivier Métais, and Pierre Comte. *Large-eddy simulations of turbulence*. Cambridge university press, 2005.
- [25] Pan, Bing, and Qiong Wang. "Single-camera microscopic stereo digital image correlation using a diffraction grating." *Optics Express* 21.21 (2013): 25056-25068.
- [26] Zalnejad, Kaveh, Seyyed Fazlollah Hossein, and Yousef Alipour. "The Impact of Livable City's Principles on Improving Satisfaction Level of Citizens; Case Study: District 4 of Region 4 of Tehran Municipality." *Armanshahr Architecture & Urban Development* 12.28 (2019): 171-183.
- [27] Zalnezhad, Kaveh, Mahnaz Esteghamati, and Seyed Fazlollah Hoseini. "Examining the Role of Renovation in Reducing Crime and Increasing the Safety of Urban Decline Areas, Case Study: Tehran's 5th District." *Armanshahr Architecture & Urban Development* 9.16 (2016): 181-192.
- [28] Yun, Chidi, et al. "The use of bilayers consisting of graphene and noble metals has been explored for biosensors that employ inverted surface plasmon resonance." *International Journal of Science and*

- Information System 12.8 (2022): 441-449.
- [29] Motalo, Kubura, et al. "Hybrid nanostructures consisting of as-grown graphene and copper nanoparticles have been developed to improve the intensity and stability of surface plasmon resonance." *International Journal of Basis Applied Science and Study* 13.24 (2022): 2561-2570.
- [30] Balen, John, et al. "Quantum plasmonic sensing is employed to experimentally measure kinetic parameters." *Journal of Basis Applied Science and Management System* 8.7 (2022): 136-146.
- [31] Sharifani, Koosha and Amini, Mahyar and Akbari, Yaser and Aghajanzadeh Godarzi, Javad. "Operating Machine Learning across Natural Language Processing Techniques for Improvement of Fabricated News Model." *International Journal of Science and Information System Research* 12.9 (2022): 20-44.
- [32] Amini, Mahyar, et al. "MAHAMGOSTAR.COM AS A CASE STUDY FOR ADOPTION OF LARAVEL FRAMEWORK AS THE BEST PROGRAMMING TOOLS FOR PHP BASED WEB DEVELOPMENT FOR SMALL AND MEDIUM ENTERPRISES." *Journal of Innovation & Knowledge*, ISSN (2021): 100-110.
- [33] Amini, Mahyar, and Aryati Bakri. "Cloud computing adoption by SMEs in the Malaysia: A multi-perspective framework based on DOI theory and TOE framework." *Journal of Information Technology & Information Systems Research (JITISR)* 9.2 (2015): 121-135.
- [34] Amini, Mahyar, and Nazli Sadat Safavi. "A Dynamic SLA Aware Heuristic Solution For IaaS Cloud Placement Problem Without Migration." *International Journal of Computer Science and Information Technologies* 6.11 (2014): 25-30.
- [35] Amini, Mahyar. "The factors that influence on adoption of cloud computing for small and medium enterprises." (2014).
- [36] Amini, Mahyar, et al. "Development of an instrument for assessing the impact of environmental context on adoption of cloud computing for small and medium enterprises." *Australian Journal of Basic and Applied Sciences (AJBAS)* 8.10 (2014): 129-135.
- [37] Amini, Mahyar, et al. "The role of top manager behaviours on adoption of cloud computing for small and medium enterprises." *Australian Journal of Basic and Applied Sciences (AJBAS)* 8.1 (2014): 490-498.
- [38] Amini, Mahyar, and Nazli Sadat Safavi. "A Dynamic SLA Aware Solution For IaaS Cloud Placement Problem Using Simulated Annealing." *International Journal of Computer Science and Information Technologies* 6.11 (2014): 52-57.
- [39] Sadat Safavi, Nazli, Nor Hidayati Zakaria, and Mahyar Amini. "The risk analysis of system selection and business process re-engineering towards the success of enterprise resource planning project for small and medium enterprise." *World Applied Sciences Journal (WASJ)* 31.9 (2014): 1669-1676.
- [40] Sadat Safavi, Nazli, Mahyar Amini, and Seyyed AmirAli Javadinia. "The determinant of adoption of enterprise resource planning for small and medium enterprises in Iran." *International Journal of Advanced Research in IT and Engineering (IJARIE)* 3.1 (2014): 1-8.
- [41] Sadat Safavi, Nazli, et al. "An effective model for evaluating organizational risk and cost in ERP implementation by SME." *IOSR Journal of Business and Management (IOSR-JBM)* 10.6 (2013): 70-75.
- [42] Safavi, Nazli Sadat, et al. "An effective model for evaluating organizational risk and cost in ERP implementation by SME." *IOSR Journal of Business and Management (IOSR-JBM)* 10.6 (2013): 61-66.
- [43] Amini, Mahyar, and Nazli Sadat Safavi. "Critical success factors for ERP implementation." *International Journal of Information Technology & Information Systems* 5.15 (2013): 1-23.
- [44] Amini, Mahyar, et al. "Agricultural development in IRAN base on cloud computing theory." *International Journal of Engineering Research & Technology (IJERT)* 2.6 (2013): 796-801.
- [45] Amini, Mahyar, et al. "Types of cloud computing (public and private) that transform the organization more effectively." *International Journal of Engineering Research & Technology (IJERT)* 2.5 (2013): 1263-1269.
- [46] Amini, Mahyar, and Nazli Sadat Safavi. "Cloud Computing Transform the Way of IT Delivers Services to the Organizations." *International Journal of Innovation & Management Science Research* 1.61 (2013): 1-5.
- [47] Abdollahzadegan, A., Che Hussin, A. R., Moshfegh Gohary, M., & Amini, M. (2013). The organizational critical success factors for adopting cloud computing in SMEs. *Journal of Information Systems Research and Innovation (JISRI)*, 4(1), 67-74.
- [48] Khoshraftar, Alireza, et al. "Improving The CRM System In Healthcare Organization." *International Journal of Computer Engineering & Sciences (IJCES)* 1.2 (2011): 28-35.